

TR-0105

AD

Reports Control Symbol
OSD - 1366

THE VISIOCEILOMETER: A PORTABLE VISIBILITY AND CLOUD CEILING HEIGHT LIDAR

JANUARY 1982

By

W. J. Lentz

Approved for public release; distribution unlimited.



US Army Electronics Research and Development Command
Atmospheric Sciences Laboratory
White Sands Missile Range, NM 88002

NOTICES

Disclaimers

The findings in this report are not to be construed as an official Department of the Army position, unless so designated by other authorized documents.

The citation of trade names and names of manufacturers in this report is not to be construed as official Government indorsement or approval of commercial products or services referenced herein.

Disposition

Destroy this report when it is no longer needed. Do not return it to the originator.

SECURITY CLASSIFICATION OF THIS PAGE *(When Data Entered)*

REPORT DOCUMENTATION PAGE		READ INSTRUCTIONS BEFORE COMPLETING FORM
1. REPORT NUMBER ASL-TR-0105	2. GOVT ACCESSION NO.	3. RECIPIENT'S CATALOG NUMBER
4. TITLE *(and Subtitle)* THE VISIOCEILOMETER: A PORTABLE VISIBILITY AND CLOUD CEILING HEIGHT LIDAR		5. TYPE OF REPORT & PERIOD COVERED Final Report 6. PERFORMING ORG. REPORT NUMBER
7. AUTHOR*(s)* W. J. Lentz		8. CONTRACT OR GRANT NUMBER*(s)*
9. PERFORMING ORGANIZATION NAME AND ADDRESS US Army Atmospheric Sciences Laboratory White Sands Missile Range, NM 88002		10. PROGRAM ELEMENT, PROJECT, TASK AREA & WORK UNIT NUMBERS DA Task No. 1L162111AH71-D0
11. CONTROLLING OFFICE NAME AND ADDRESS US Army Electronics Research and Development Command Adelphi, MD 20783		12. REPORT DATE January 1982 13. NUMBER OF PAGES 46
14. MONITORING AGENCY NAME & ADDRESS*(if different from Controlling Office)*		15. SECURITY CLASS. *(of this report)* UNCLASSIFIED 15a. DECLASSIFICATION/DOWNGRADING SCHEDULE

16. DISTRIBUTION STATEMENT *(of this Report)*

Approved for public release; distribution unlimited.

17. DISTRIBUTION STATEMENT *(of the abstract entered in Block 20, if different from Report)*

18. SUPPLEMENTARY NOTES

19. KEY WORDS *(Continue on reverse side if necessary and identify by block number)*

Visibility
Ceiling
Slant visual range
Extinction
Lidar

20. ABSTRACT *(Continue on reverse side if necessary and identify by block number)*

A hand-held visibility and cloud ceiling height lidar based on the AN/GVS-5 laser rangefinder will be described. This militarized, battery-operated lidar automatically calculates visibility based on the Klett solution of the lidar equation. Visibilities from 10 to 199,999 m and cloud ceiling heights from 50 to 3000 m may be calculated. The measurements from this visioceilometer have been favorably compared to visibilities derived from larger lidars, balloon-borne particle counters, and transmissometers. The entire unit weighs less than 14 lb.

DD FORM 1 JAN 73 1473 EDITION OF 1 NOV 65 IS OBSOLETE

SECURITY CLASSIFICATION OF THIS PAGE *(When Data Entered)*

ACKNOWLEDGMENTS

I would like to thank Don Foiani and Ed Measure for their helpful comments on this manuscript. I should also like to thank Jim Lindberg for allowing me to use figure 8, which he prepared for a comparison of the visioceilometer to extinction calculated from a balloon-borne particle counter.

CONTENTS

LIST OF TABLES..... 6

LIST OF FIGURES..... 6

INTRODUCTION..... 7

VISIBILITY DEFINITION..... 7

VISIOCEILOMETER DESCRIPTION..... 8

TRANSIENT RECORDER..... 9

LIDAR ANALYSIS..... 10

LOW VISIBILITY CASE..... 12

HIGH VISIBILITY CASE..... 12

EXPERIMENTAL RESULTS..... 15

APPLICATIONS OF THE VISIOCEILOMETER..... 15

TABLE..... 17

FIGURES..... 18

LIST OF TABLES

1. Visioceilometer Characteristics..... 17

LIST OF FIGURES

1a. Visioceilometer photograph with battery..... 18

1b. Visioceilometer block diagram..... 18

2. Extinction vs range for various boundary value estimates..... 19

3. Theoretical lidar returns for various boundary value estimates..... 19

4. Normalized theoretical lidar returns..... 20

5. Experimental lidar returns for various boundary value estimates..... 20

6. Extinction vs range for various near field starting points..... 21

7. Single-shot visioceilometer extinction vs range for fog in Meppen, Germany..... 21

8. Visioceilometer extinction compared to extinction calculated by balloon-borne particle counter in Meppen, Germany..... 22

INTRODUCTION

In recent years lidar (Light Detection and Ranging) has made significant technical and theoretical advances. A lidar no longer need be the cumbersome and fragile set of lenses and electronics that it was at its inception. A lidar may now be small, light, rugged, battery-operated, simple to use, and completely self-contained. Tedious data processing and external inputs are no longer needed to reduce a lidar return to visibility. Such a lidar has been developed by Atmospheric Sciences Laboratory (ASL) to support aircraft landings, optically dependent weapon firings, and operations where the atmospheric extinction needs to be remotely measured. Since the lidar measures visibility and cloud ceiling height, it has been dubbed a visioceilometer. This paper describes the characteristics of the XE-2 visioceilometer shown in figure 1a and compares its measurements to more conventional visibility-measuring devices.

VISIBILITY DEFINITION

Visibility must be precisely defined before a measurement of visibility is made. Furthermore, the definition must be constructed in such a way that what a machine measures can be related to what the eye sees. Visibility observed by the human eye is a very complex parameter depending on may factors besides the obscuring medium. For example, a standard airport transmissometer is said to measure visibility, but it actually measures transmission between two points. Under the same conditions it will indicate the same visibility at day or night, even though the human eye might define the visibility quite differently. Middleton[1] has defined the meteorological range or visual range V_r to be

$$V_r = \frac{-\ln(0.02)}{\sigma} \qquad (1)$$

where 0.02 is the minimum contrast threshold for standard target detection with the human eye, and σ is the volume extinction coefficient which may be measured by machine.

One of the problems with using equation (1) is that the visibility may be very different than that predicted by the equation. For example, suppose a transmissometer makes a measurement of extinction over a 3 km path with the receiver immersed in 100 m of a fog bank. The average extinction measured over the entire path may predict a lower visibility than the distance to the fog bank. Equation (1) will generally be in error if the turbid medium has

---

[1]Middleton, W. E. K., 1963, Vision Through the Atmosphere, Toronto Press, Toronto, Canada.

significant variations in extinction along the path in which V_r is measured. A better definition of visibility as measured by an instrument over a path length having a variable σ is given by[2]

$$3.912 = \int_0^{V_{rm}} \sigma(r)dr \qquad (2)$$

where V_{rm} is the range at which the total extinction is 3.912, corresponding to a contrast threshold of 0.02. If the extinction is so low that the measurement cannot be made over the full visual range V_r, then the best extrapolation of visibility would be given by equation (1).

Equations (1) and (2) can be related to observer-defined visibility if proper consideration is made of the ambient lighting conditions. The lidar can return the value of σ measured over the length of the lidar return, so visibility as measured by the lidar will be defined as in equation (1) or (2) as appropriate for the rest of this discussion.

VISIOCEILOMETER DESCRIPTION

The visioceilometer is a lidar consisting of two interconnected units which operate together to produce a measurement of visibility or cloud ceiling height. The modified rangefinder, called the optical unit (OU), was built under a joint development effort with Night Vision and Electro-Optics Laboratory[3] by RCA Corporation. A separate transient recorder and microprocessor make up the signal processing unit (SPU), engineered and developed through contract with Lawrence Livermore Laboratory. The laser source and receiver are part of a modified AN/GVS-5 laser rangefinder currently in production for the US Armed Forces.

The functional diagram of the visioceilometer is shown in figure 1b. A laser emits a single 1.06μm pulse into a very narrow beam, and the atmosphere scatters the light back into the receiver optics according to the turbidity. The received flux is detected by a silicon photoavalanche detector, and the signal is compressed by a logarithmic amplifier. The output of the laser is monitored by a temperature-compensated PIN photodiode. Both the monitor pulse and the lidar return signal are sent by coaxial cable to the SPU, where they are digitized and analyzed. A CMOS microprocessor analyzes the return for visibility or cloud ceiling height, according to the switch setting on the

---

[2]Hermann, H., et al, 1974, "Lidar Measurements of Atmospheric Visibility," Alta Frequenza, vol 9, p 732.

[3]Bonner, Robert S., and William J. Lentz, 1979, The Visioceilometer: A Portable Cloud Height and Visibility Indicator, ASL-TR-0042, US Army Atmospheric Sciences Laboratory, White Sands Missile Range, NM.

OU, and the result is displayed in the eyepiece of the OU under microprocessor control. The microprocessor turns itself off after each calculation to conserve power until the next laser monitor pulse starts the digitization and analysis process again. The detailed physical and optical characteristics of the visioceilometer are listed in table 1.

Visibility or cloud ceiling height is calculated automatically, and the result is displayed in the eyepiece in a 5-digit numerical display. The function is indicated by an LED with a C-shaped mask for ceiling or V-shaped mask for visibility. The visibility or ceiling result is displayed in the eyepiece for 5 s before the display is automatically turned off to conserve power. A refresh button may be pushed to redisplay the last ceiling or visibility value in the eyepiece at any time until the system power is turned off or the laser is fired again.

The OU has a two-position laser fire switch, a standard feature of the AN/GVS-5 laser rangefinder. When the switch is depressed halfway, the laser flash lamp capacitor charges to prepare for laser firing. The laser then fires instantly when the fire button is depressed completely. This feature is used to conserve power in the SPU by turning on the microprocessor only when the fire button is depressed at least halfway. When the fire button is completely depressed, the transient recorder starts clocking to get ready to digitize when a laser monitor pulse is received. Analysis of the lidar return only occurs when a laser monitor signal within the range 0.75 V $\pm$ 0.25 V is received. This limit precludes the possibility of trying to analyze lidar returns produced by a laser operating outside of normal tolerance limits.

The OU and SPU run on separate BB-516 batteries housed in the SPU. These AN/GVS-5 24-V rechargeable NiCd cells (about the size of a C cell) will provide at least 100 visibility calculations between chargings. The LED display will indicate a low battery state in the OU eyepiece. Since it contains both batteries, the SPU weighs about 8 lb whereas the OU weighs only 5 lb.

TRANSIENT RECORDER

The innovation that allows an inexpensive, low power visioceilometer to be built is in the transient recorder. A charge-coupled device (CCD) was chosen to slow down the wide bandwidth lidar return so that a relatively high accuracy, low power, analog to digital converter (ADC) could digitize the return. The CCD-based transient recorder allows the 23µs lidar return to be converted to a 46 ms pulse, which is easier to digitize. The CCD samples the lidar return at a 20-MHz rate, which corresponds to a sample every 7.5 m along the lidar beam path. A total of 455 samples thus corresponds to a total sampled return of 3.3 km.

The digitized lidar return is processed into cloud ceiling height or visibility by an RCA 1802 CMOS microprocessor and an arithmetic processing unit

(AMD 9511) using the Klett[4] method of analysis. The microprocessor preprocesses data by removing baseline shift, nonlinearities, CCD errors, and laser output variations. The arithmetic processing unit does 32-bit floating point arithmetic and computes functions, such as the logarithm, in a mere fraction of the time that the CMOS microprocessor alone would take.

The laser energy monitor pulse is used to correct the lidar return or amplitude variations in the laser output and to start the digitization process. Since it is difficult to start a 20-MHz clock synchronously with the start pulse, a delay line is used to measure the fixed phase shift between the start pulse and the clock at each laser shot. The stored time delay is used in the algorithm to more accurately remove the attenuation due to range. An acceptable error of 0.75 m or 5 ns is produced in this manner in the first analyzed point at 100 m, but the error of 7.5 m or 50 ns produced without the stored delay would have been unacceptable.

In the SPU, an internally generated ramp pulse is fed to the CCD and digitized as soon as the laser charge button is pressed. The resultant digitized values allow one to correct the CCD nonlinearities and to check the transient recorder for proper operation. When the laser return has been digitized, the transient recorder is shut off to save power while the microprocessor calculates visibility or cloud ceiling height.

The SPU also has a programmable serial data output capability so that the raw digitized lidar return may be more extensively analyzed by a larger computer if more than the visibility is desired as output. When an external plug is connected to the serial output, RS232 standard format serial data are generated at 9600 Bd, so that they may be stored and analyzed for such information as extinction vs range. When the external plug is not connected, no serial output data are generated. The capability of providing serial data in a standard format allows a variety of types of information to be communicated to external devices, improving the versatility of the visioceilometer.

LIDAR ANALYSIS

A significant advance recently has been made which allows the conversion of lidar returns to extinction as a function of range. The Klett method is a new analytical solution to the lidar equation which lacks the instability that has plagued approximate methods. Klett's method allows the calculation of the extinction efficiency with distance no matter what the degree of inhomogeneity, as long as Klett's assumptions are valid. All that is required is an estimate of the extinction at the furthest point of the lidar return, and this can be determined from the lidar calibration or an independent device.

---

[4]Klett, James D., 1980, On the Analytical Inversion of Lidar Returns from an Inhomogeneous Atmosphere, ASL-CR-80-0008-3, US Army Atmospheric Sciences Laboratory, White Sands Missile Range, NM.

The lidar equation representing the returned flux produced by a pulsed laser is given by:

$$P(r) = P_o c \frac{A\beta(r)F(r)\tau}{2r^2} \exp\left[-2\int_0^r \sigma(r')dr'\right] \quad (3)$$

where $P(r)$ is the flux received by the lidar as a function of time or range r, P_o is the transmitted power in a pulse of width τ, A is the effective receiver area, $\beta(r)$ is the volume backscatter coefficient at r, F includes the system sensitivity and geometric crossover efficiency, and $\sigma(r)$ is the volume extinction coefficient. The pulse of energy from the laser transmitter is attenuated by the extinction, which varies with range until it reaches a point r. The volume backscatter coefficient then determines the fraction of energy which is scattered back into the receiver from the point r. The Klett[4] solution is derived in the following manner.

Since there is no real information in the r^2 term, and since the exponent is an inconvenient complication, the term $S(r)$ will be defined:

$$S(r) = \ln[r^2 P(r)] \quad (4)$$

It has been shown that there is often a relationship between $\beta(r)$ and $\sigma(r)$ of the form:[4]

$$\beta(r) = C\sigma^k(r) \quad (5)$$

By taking the derivative of $S(r)$ and using the lidar equation and equation (5), one has:

$$\frac{dS}{dr} = \frac{k}{\sigma}\frac{d\sigma}{dr} - 2\sigma \quad (6)$$

The solution to an equation of this form is well-known, and a new stable formulation has been derived by Klett:

$$\sigma(r) = \frac{\left[\exp\ (S - S_m)/k\right]}{\sigma_m^{-1} + 2/k\int_r^{R_m} \exp\left[(S - S_m)/k\right]dr'} \quad (7)$$

---

[4]Klett, James D., 1980, On the Analytical Inversion of Lidar Returns from an Inhomogeneous Atmosphere, ASL-CR-80-0008-3, US Army Atmospheric Sciences Laboratory, White Sands Missile Range, NM.

Where $r_m > r$ is the new calibration point, $S_m = S(r_m)$, and $\sigma_m = \sigma(r_m)$. This solution is easily computed from the known values of P(r), with k deduced from theoretical calculations or experimental measurements and σ_m derived by other means.

LOW VISIBILITY CASE

One unexpected feature of the Klett solution is that for moderately low visibility the solution is not dependent on the estimate for σ_m.[4] In fact it converges to the correct value in just a short distance from r_m. Previous solutions were either unstable or so approximate as to be unstable in many interesting cases. The convergence can be seen in figure 2, which shows the same lidar return analyzed by the Klett solution using different estimates of σ_m. In a relatively short distance, beginning at r_m and working back to r_o, the true solution is deduced from nothing more than the shape of the lidar return. In the particular example chosen in figure 2, the extinction was constant with range, but the convergence to the correct answer occurs regardless of the shape of the true extinction as a function of range. This behavior is explained by the fact that as the difference between r and r_m grows, the integral in the denominator of equation (7) grows. The integral will eventually grow to the point that the value of σ_m is relatively unimportant and nearly any reasonable value can be used as a boundary value.

HIGH VISIBILITY CASE

The convergence of the Klett solution is very slow for high visibilities, so a new method of estimating the boundary value must be used. The simplest method is to relate the magnitude of S(r) as well as its shape to the solution $\sigma(r)$. Let us consider the measured lidar return:

$$\ln[P(r)] = \ln(K) + \ln(C) + \ln[\sigma(r)] - 2\ln(r) - 2\bar{\sigma}\, r \qquad (8)$$

where $\beta(r) = C\sigma(r)$ and $k = 1$. K is, for simplicity, an aggregate of all of the system constants which can be measured or calculated. The last term is:

$$\bar{\sigma}\, r = \int_0^r \sigma(r')dr' \qquad (9)$$

---

[4]Klett, James D., 1980, On the Analytical Inversion of Lidar Returns from an Inhomogeneous Atmosphere, ASL-CR-80-0008-3, US Army Atmospheric Sciences Laboratory, White Sands Missile Range, NM.

Neglecting the constants in equation (8), one has a new equation:

$$Z(r) = \ln[\sigma(r)] - 2\ln(r) - 2\bar{\sigma}\, r \qquad (10)$$

For ranges beyond the crossover range of the receiver and transmitter fields of view, the system constant K is unchanging. The ratio β/σ may change as the atmosphere changes, producing a varying C. This variation does not produce a serious error, since a change in C is reduced in magnitude by the ln function. For example a factor change of 5 in C produces a factor change of only 1.61 in ln(C). Moreover, the ln(K) is usually larger than ln(C), further reducing the resultant error. In lieu of theoretical calculations, it will be assumed that C is constant for fogs. It should be remembered that the constant C is only used for high visibilities when the self-convergence of the Klett[4] solution is not adequate.

The correct boundary value may be chosen to produce an accurate extinction curve by measuring the simultaneous lidar return and transmission at 1.06μm and applying the Klett method. The difference between equations (8) and (10) gives the unknown constants which allow measurements to be made independent of the transmissometer. Once the constants are known, all experimental returns may be reduced to equation (10) and compared to the form produced by the Klett solution. When the experimental curve matches the solution curve, the correct boundary value has been identified.

Let us consider the set of curves in figure 3. The three curves correspond to equation (4) for three boundary values used in the Klett solution. If the boundary value is too large, the curve will lie above the measured curve at every point, and if σ_m is too small, the theoretical curve produced by the Klett formula will lie below the measured curve at every point. Inasmuch as these values may be positive or negative, corresponding to the magnitude of ln[P(r)], it is convenient to normalize the curves to a common point, as in figures 4 and 5, to reduce the magnitude of the variation due to different boundary values. A simple Newton's method iteration may then be applied to allow rapid convergence to the correct boundary value.

A comparison between the curves at only one point would not be desirable because the lidar return contains noise as well as valid signals, and there is no easy way to know just how large the error is at only one point. A better approach is to sum the S(r) values and the Z(r) values over the same interval. The average thus produced is much more stable than just one point, and the average may be used in a Newton's method iteration to produce a very accurate boundary value estimate. The resulting σ(r) produced by the Klett

---

[4]Klett, James D., 1980, On the Analytical Inversion of Lidar Returns from an Inhomogeneous Atmosphere, ASL-CR-80-0008-3, US Army Atmospheric Sciences Laboratory, White Sands Missile Range, NM.

method may vary several orders of magnitude along r and still be accurate at every point. Specifically, the next boundary value iteration is given by:

$$\sigma_2 = \sigma_1 - f(\sigma_1)/f'(\sigma_1)$$

where

$$f(\sigma_1) = \Sigma(S_m - S_t)$$

and

$$f'(\sigma_1) = \frac{\Sigma S_t(\sigma_1) - \Sigma S_t(\sigma_0)}{\sigma_1 - \sigma_0}$$

and S_t is the theoretical S(r),

and S_m is the measured S(r).

For high visibilities, the magnitude of σ is much smaller than the magnitude of $\ln[\sigma(r)]$. Therefore, the boundary value estimates and the σ curves agree to a high degree of accuracy. For the case of low visibilities in which the last term in equation (8) cannot be neglected, the self-convergence of the Klett[4] solution eliminates the need for the Newton's boundary value estimate.

Most real lidars do not see returns from the exit of the laser to the limit of detectable signal. There is a short region of optical crossover or defocus which prevents data from being used for about 100 m. If the neglected data cause significant error, the method will not be reliable for large changes in σ. Consider the two σ curves in figure 6, produced from measured lidar data using the previously described Klett solution and area method for a boundary value. The two curves are extinction vs range produced from two analyses of the same lidar return. Although one curve begins at point 15 and the other at point 20, the curves match, indicating a lack of sensitivity to the neglected points. This is both a necessary and fortunate result, because it is extremely difficult to design a lidar that is weatherproof and receives all of the light scattered in the near field without losing light in the far field.

It would not have been possible to calculate identical curves in figure 6 without the Klett method, because a large haze peak was virtually centered on the lidar. The air became clearer as the pulse moved away from the lidar. The slope method would have produced an effective visibility of much less than 1 km, but no visible obscurant could be seen. The average visibility during this period was about 26 km, as measured by a long-path transmissometer.

---

[4]Klett, James D., 1980, On the Analytical Inversion of Lidar Returns from an Inhomogeneous Atmosphere, ASL-CR-80-0008-3, US Army Atmospheric Sciences Laboratory, White Sands Missile Range, NM.

We now have a general method of determining $\sigma(r)$ over the range of the lidar return in high and low visibilities. It makes use of the absolute value of the signal, which is not normally used in Klett's equation (7). By comparing the measured $\ln[P(r)]$ to the $Z(r)$ calculated from the $\sigma(r)$ produced by the Klett solution, the Klett method may be reapplied several times to produce $\sigma(r)$ as accurately as the system constants and lidar returns are known. C and k values may be measured independently or obtained from theoretical studies.

EXPERIMENTAL RESULTS

ASL recently conducted a field test in Meppen, Germany, where opportunities existed to test the lidar theory against extinction measurements made by balloon-borne particle counters. Figures 7 and 8 show the extinction obtained by firing the visioceilometer vertically into fogs or low clouds at the Meppen experiment, which ASL conducted from October to December of 1980. Balloon-borne particle counters were used to calculate the extinction at 1.06μm, as a function of altitude. These values generally agreed to within a factor of two with the values produced by the visioceilometer. Furthermore, the visioceilometer extinction curves show much more structure than the balloon counters, because the lidar is virtually instantaneous. The agreement is rather good, especially when one considers that the lidar was not pointing exactly at the balloon because the balloon could not be seen.

The data shown in figures 7 and 8 were recorded with the lidar pointing vertically into fog or clouds of increasing density. In some cases the lidar penetrated one layer of obscurant and returned information about a second layer. Since the extinction values were extremely high, it was not possible to tell whether the lidar penetrated the second layer into clear air. It is more likely, however, that the lidar simply ran out of energy, and the last four sample points should therefore not be regarded very seriously.

APPLICATIONS OF THE VISIOCEILOMETER

The visioceilometer has immediate tactical use as a slant path visual range indicator at remote airfields where visibility and cloud ceiling height are required but where conventional instruments are too inconvenient. Indeed, the visioceilometer may be the only portable instrument which can directly measure slant visual range along the glide path of the aircraft. Since the visioceilometer is completely automatic and records visibility even when there are no reference objects in sight, a reliable, repeatable measurement may be made by an untrained observer. These measurements could be made at Army Division Artillery meteorological sections in lieu of visual observations and ceiling balloons, particularly at night when such measurments are difficult.

Naval shipboard uses include visibility, which is especially difficult to measure at sea because of the lack of reference visibility objects. The visioceilometer can be programmed to neglect the ship-generated effluent plume which makes shipboard transmissometers difficult to use. A vertical measurement of visibility may be made to determine whether the ship is visible from above by aircraft. Regular use of the visioceilometer would provide a general marine-visibility data base, which would be of tactical use in planning ship deployment.

Guided munitions such as Copperhead rely on optical sensors to locate and destroy a target. The visioceilometer could be used to measure the visibility in the target area so that rounds would not be expended uselessly. A related nontactical use would be to characterize the atmosphere when test firings are made of optically guided rounds, so that better performance assessments could be made.

The visioceilometer could also be used as a general research tool in lieu of more difficult and far more expensive balloon-borne particle counter measurements. With external RS232 devices, data for computation of extinction vs range can be stored and analyzed later for detailed characterization of the atmosphere.

The visioceilometer would allow measurement of smokestack plume opacity even though the laser might not penetrate the plume with sufficient energy to produce a return from the clear air on the distant side. The Klett[4] method works especially well in high opacity cases because the boundary value selection is self-converging. It offers the advantage of measuring opacity at night, when there is a temptation to produce dense plumes because of the difficulty of making nighttime observations. Although the visioceilometer might not measure the transmission completely through the plume, it would set a lower bound on the opacity, which would encompass several decades of attenuation.

The visioceilometer could also be integrated into the meteorological sensor system of the Remote Automatic Weather Set (RAWS) or AN/TMQ-30 to provide visibility and cloud ceiling height information. In this application, sensors would be placed in forward areas of the battlefield by a ground sensor platoon. These unattended weather stations would transmit data automatically by a radio link to a master station, which would collect data from a number of RAWS units. The self-contained feature of the visioceilometer data analysis would lend itself readily to the incorporation of the visioceilometer in a variety of devices such as the RAWS.

---

[4]Klett, James D., 1980, On the Analytical Inversion of Lidar Returns from an Inhomogeneous Atmosphere, ASL-CR-80-0008-3, US Army Atmospheric Sciences Laboratory, White Sands Missile Range, NM.

TABLE 1. VISIOCEILOMETER CHARACTERISTICS

Beam divergence	1.0 mrad
Receiver field of view	3.0 mrad
Laser energy	13 mJ average at 1.06 m
Pulse half-width	6 ns
Receiver aperture	50 mm
Laser exit diameter	16 mm
Optics axis separation	50 mm
Full crossover range	80 m
Log A slope	10 mV/dB
Log A zero	80μV
Detector noise level	2×10^{-10}W
Laser monitor output	0.75 V ± 0.25 V
Sample rate	20 MHz
A/D converter	10 bits in 2μs
Sample device	455 sample Dual Channel CCD Fairchild #CCD 321
Weight	5 lb OU 8 lb SPU
Size	6 x 2 x 6 in. OU 6 x 4 x 6 in. SPU
Power	Two 24-V NiCd batteries
Number of shots	100 minimum
Operating temperature	-5° to 60°C (prototype)
Sample range	3.3 km

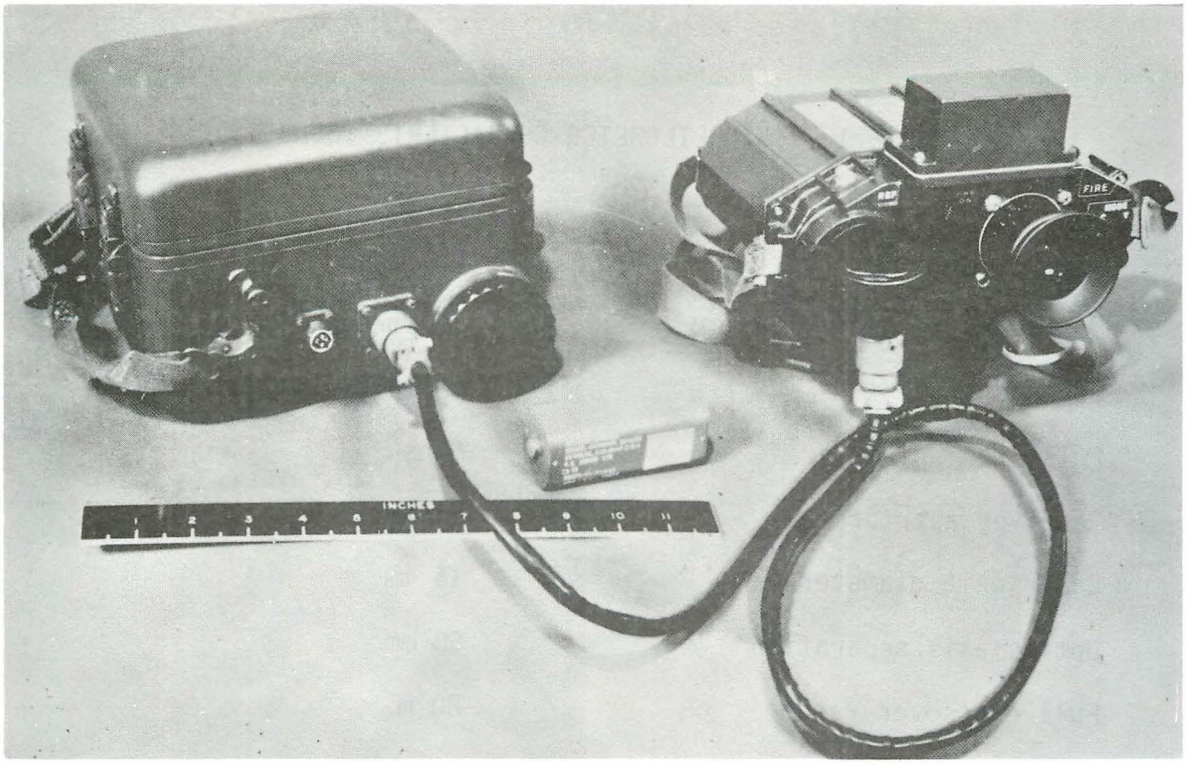


Figure 1a. Visioceilometer photograph with battery.

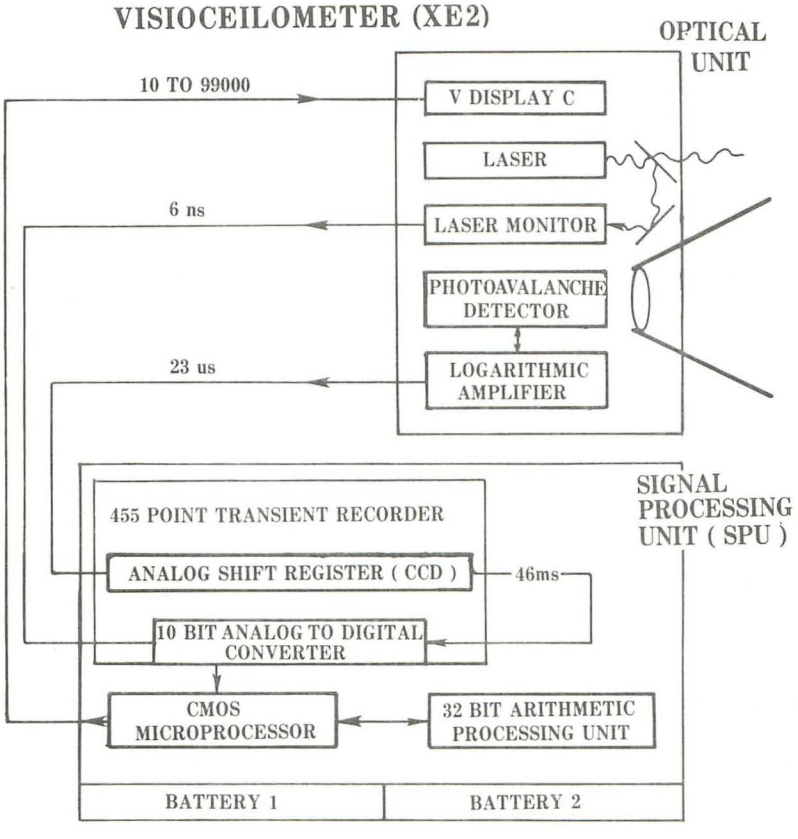


Figure 1b. Visioceilometer block diagram.

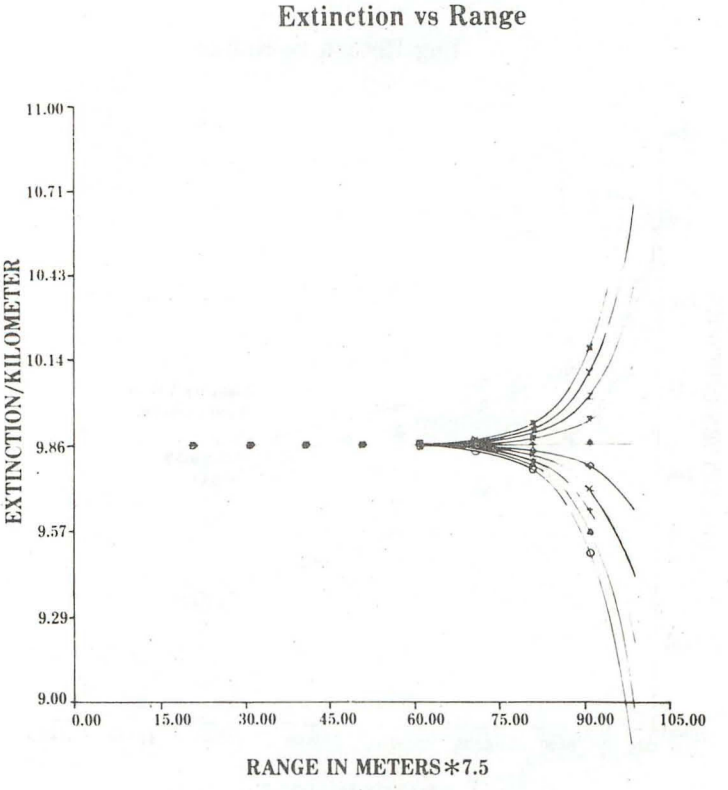


Figure 2. Extinction vs range for various boundary value estimates.

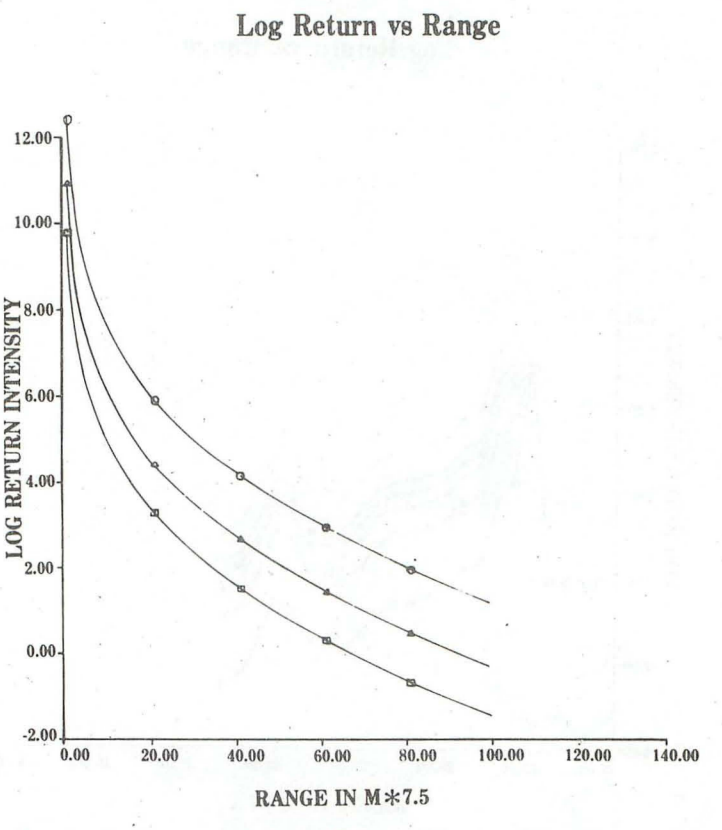


Figure 3. Theoretical lidar returns for various boundary value estimates.

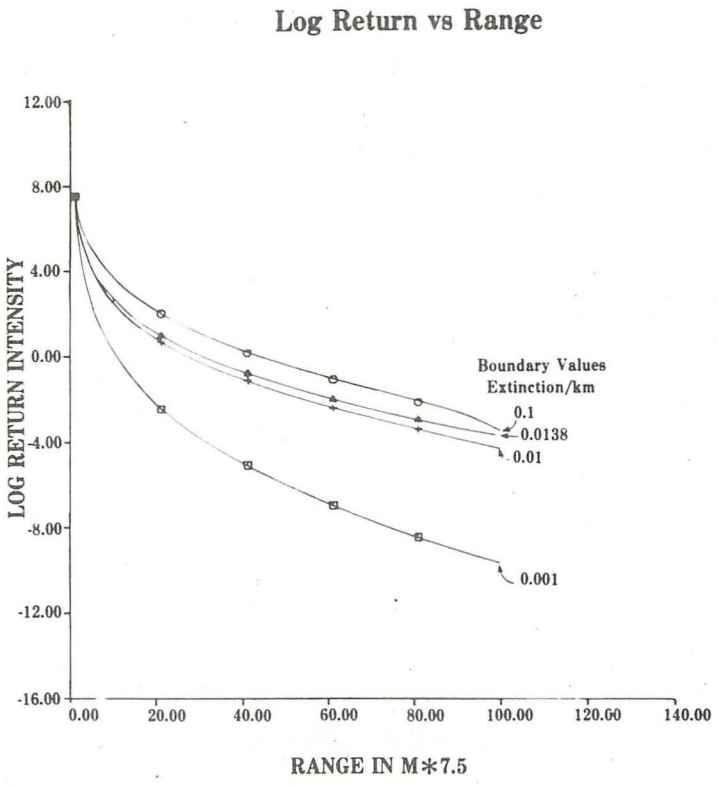


Figure 4. Normalized theoretical lidar returns.

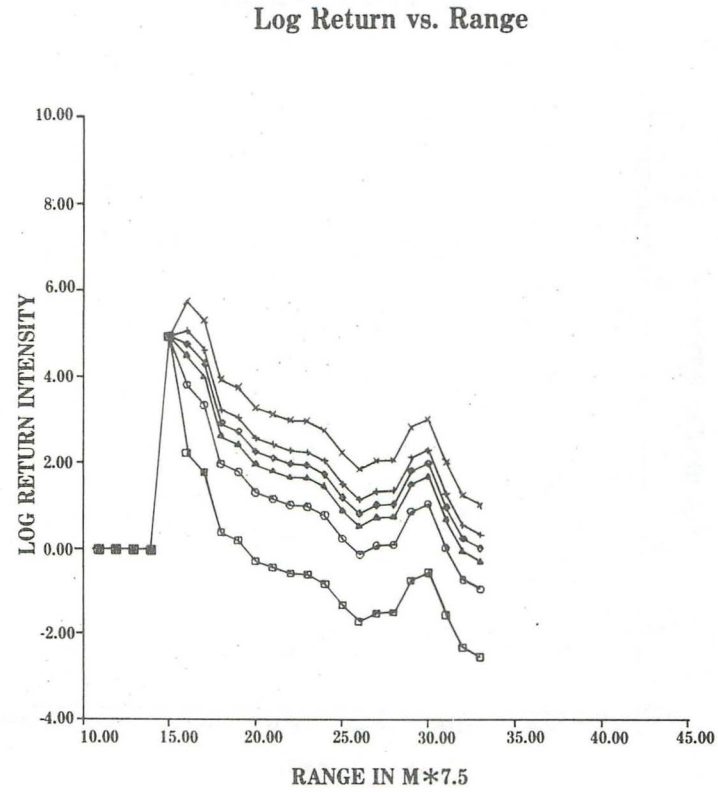


Figure 5. Experimental lidar returns for various boundary value estimates.

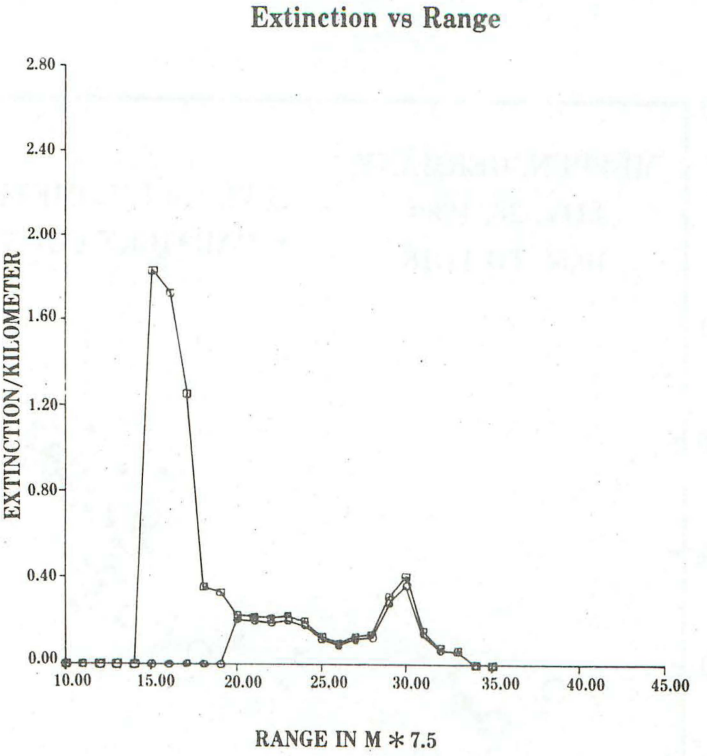


Figure 6. Extinction vs range for various near field starting points.

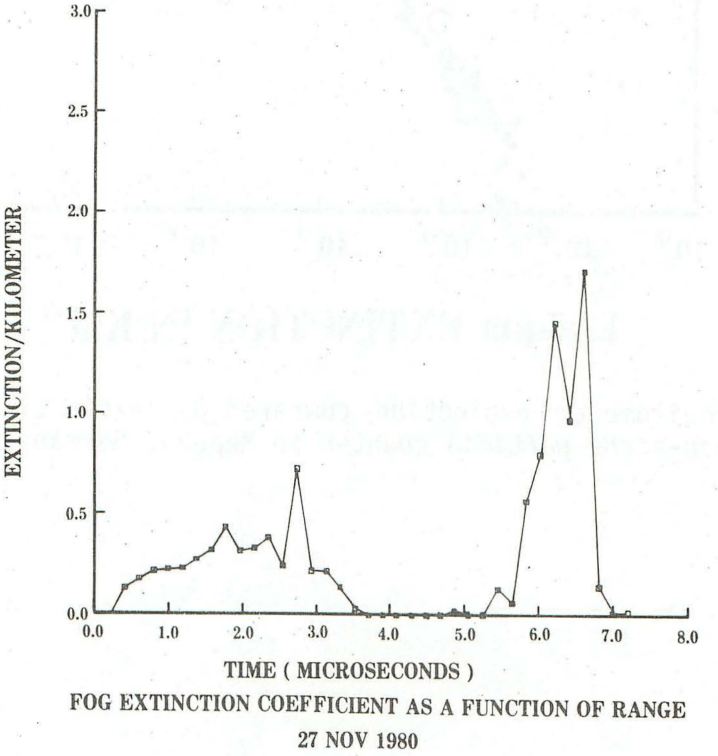


Figure 7. Single-shot visioceilometer extinction vs range for fog in Meppen, Germany.

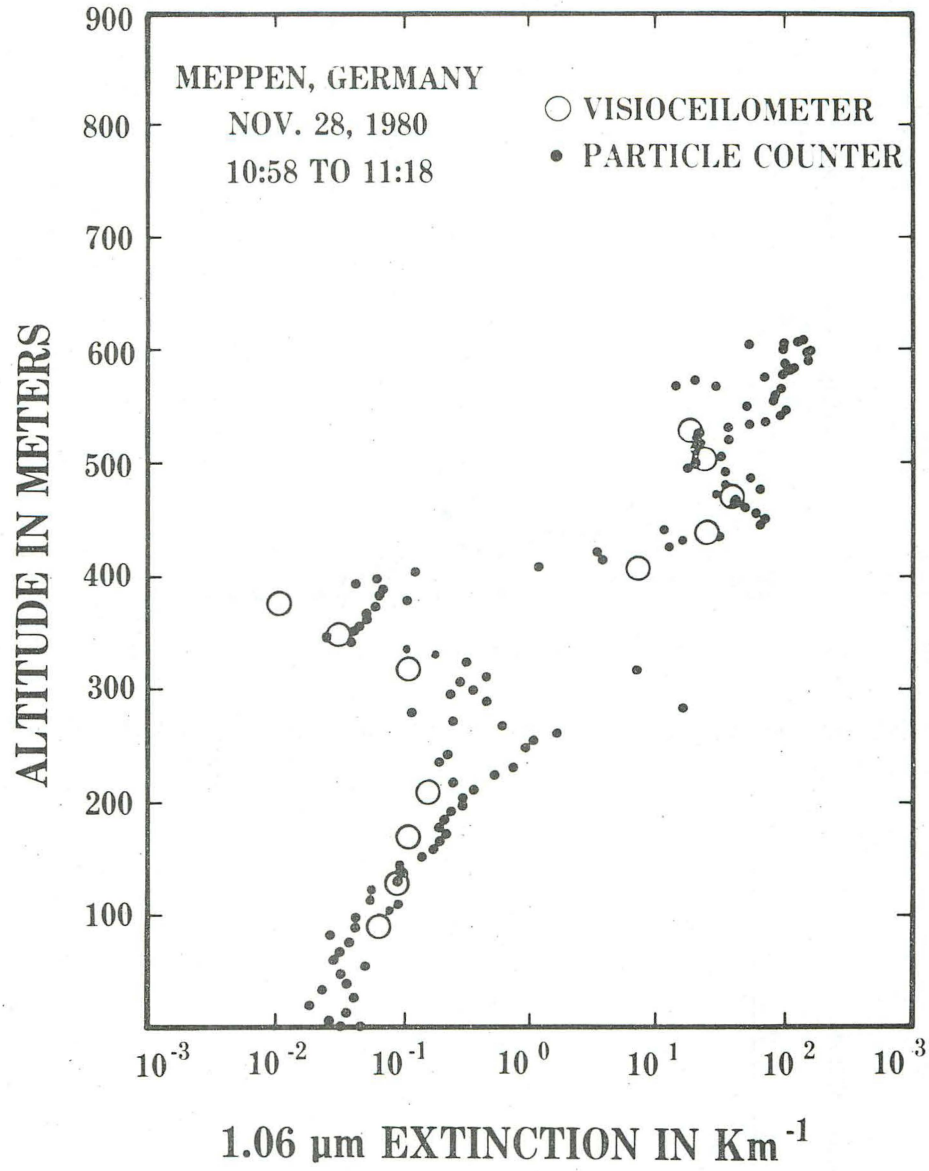


Figure 8. Visioceilometer extinction compared to extinction calculated by balloon-borne particle counter in Meppen, Germany.